An Analytical Solution for Estimating the Effect of Soil-Structure Interaction on 3D Vibration Natural Frequency of Reinforced Retaining Walls

Alireza Darvishpour[1], Ali Ghanbari[*2], Seyyed Ali Asghar Hosseini[3] , Masoud Nekooei[1]

1. Department of Civil Engineering, Science and Research Branch, Islamic Azad University, Tehran, Iran
2. Department of Civil Engineering, Kharazmi University, Mofatteh Avenue,
3. Department of Mechanical Engineering, Kharazmi University, Tehran, Iran
4. Department of Civil Engineering, Science and Research Branch, Islamic Azad University, Tehran, Iran

[DOR: 20.1001.1.22286837.1398.13.5.1.0]

Abstract

One of the effective parameters in the dynamic behavior of reinforced soil walls is the fundamental vibration frequency. In this paper, analytical expressions for the first three natural frequencies of a geosynthetic reinforced soil wall are obtained in the 3D domain, using plate vibration theory and the energy method. The interaction between reinforced soil and the wall is also considered by modeling the soil and the reinforcement as axial springs. The in-depth transverse vibration mode-shapes, which were impossible to analyze via 2D modeling, are also analyzed by employing plate vibration

[*]Corresponding author ghanbari@khu.ac.ir

theory. Different behaviors of soil and reinforcements in tension and compression are also considered for the first time in a 3D analytical investigation to achieve a more realistic result. The effect of different parameters on the natural frequencies of geosynthetic reinforced soil walls are investigated, including the soil to reinforcement stiffness ratio, reinforcement to wall stiffness ratio, reinforcement length, backfill width and length to height ratio of the wall, using the proposed analytical expressions. Finally, the results obtained from the analytical expressions proposed are compared with results from the finite element software Abaqus and other researchers' results, showing that the proposed method has high accuracy. The proposed method will be a beginning of the 3D analytical modeling of reinforced soil walls.

Keywords: Analytical method; Reinforced Retaining Wall; Natural Frequency; Shape Mode; 3D Vibration.

Introduction

Geosynthetic-reinforced soil retaining walls represent one of the most applicable geosynthetic systems used in civil engineering due to their suitable seismic behavior. Thus, great effort has been put into analyzing these types of reinforced walls so far. In the early 1990s, Japanese researchers invented a reinforced retaining wall named geosynthetic-reinforced soil-retaining wall with full-height rigid concrete facing (GRS-FHR) (Tatsuka et al. [1]). Figure 1 shows a perspective view of a geosynthetic-reinforced retaining wall. After the Hygo-ken Numbu earthquake, Japanese researchers studied the seismic behavior of the GRS-FHR walls. The results showed very satisfying behavior of these reinforced soil walls compared with walls without reinforcement while facing the

[DOR: 20.1001.1.22286837.1398.13.5.1.0]

earthquake; thus, these walls were developed and used increasingly. Various investigations of the dynamic behavior of different structures, including obtaining the natural frequency, have been conducted.

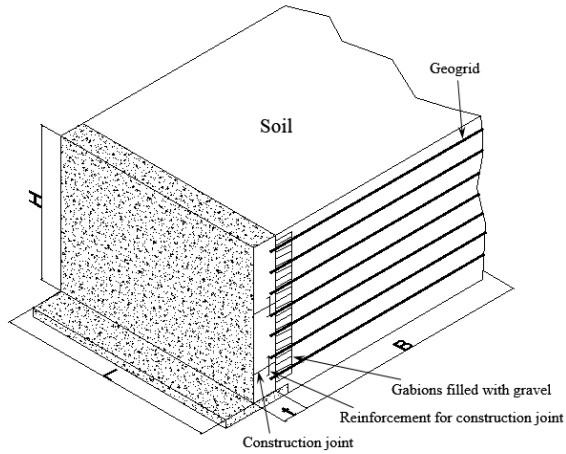

Figure 1. Schematic view of GRS-FHR wall

Obtaining the natural frequency of civil structures, such as building structures and fluid storage tanks, was performed by using modeling techniques such as concentrated mass modeling. However, to model structures such as retaining walls, continuous mass modeling is suggested to obtain more accurate results. Two of the most important parameters affecting a distributed mass system's behavior, such as a reinforced soil retaining wall, are soil-wall interaction and the interaction that exists between the reinforcements and the retaining wall, which has to be considered in both numerical and analytical modeling to achieve more precise results. A considerable analytical method for modeling the interaction between reinforced soil and a wall and its effect on the natural frequency has not yet been proposed.

All methods proposed up to now are based on the 2D modeling of wall-soil systems, which completely ignores the in-depth transverse vibration

[DOR: 20.1001.1.22286837.1398.13.5.1.0]

modes and neglects the different behaviors of reinforcement under tension and compression in the 3D domain. Thus, the results obtained from these methods are less accurate.

In this paper, the free vibration frequency of a reinforced soil retaining wall is analyzed in the 3D domain by invoking the plate vibration theory. The interactions between the wall, soil and reinforcements are also considered using axial springs. The different behaviors of the reinforcement are considered in this analytical procedure, and the tensile behavior of the soil is excluded in this study to achieve more realistic results. New analytical expressions for obtaining the three first natural frequencies of the geosynthetic reinforced soil walls are proposed using the energy method. The main purpose of this paper is to provide a 3D analytical solution for estimating the free vibration frequencies of reinforced-soil walls by considering the real behavior of the soil and reinforcement. Nevertheless, the model can be extended to evaluating seismic responses during forced vibration analyses.

Review of past studies

Many different methods have been introduced to analyze the seismic behavior and investigate the free vibration natural frequency of reinforced and non-reinforced retaining walls, including numerical, analytical and experimental methods. Matsu and Ohara [2], Wood [3], Scott [4] and Wu [5] proposed an analytical expression to calculate the fundamental frequency of a wall based on two parameters: backfill height and backfill shear wave velocity. Matsu and Ohara [2] defined two boundary limits and claimed that the main procedure is located between these two limits. Wood [3] proposed an applicable method for calculating the fundamental

[DOR: 20.1001.1.22286837.1398.13.5.1.0]

frequency of the embedded soil between two rigid retaining walls, which essentially involved solving a boundary condition problem. Scott [4] calculated the fundamental frequency of a wall by modeling the wall as a shear beam and attaching it to a Winkler spring. Yeh [6] also considered the translational and rotational vibration modes by invoking a model similar to that of Scott [3] and used the Galerkin method to solve the partial differential equations of the wall. Rigidity of the wall is an important and substantial base of all the methods mentioned above, which are based on shear beam theory. Thus, Jain and Scott [7] inserted the wall's flexibility into their calculations. Generally, most of the analytical models proposed so far are in the 2D domain. In these models, interaction between reinforcements and the wall is completely neglected or there is no difference between the tension and compression behavior of the reinforcement.

Elgamal et al. [8] studied the 3D behavior of a wall by instrumenting the retaining wall and recording the responses of the soil-wall system to a wide range of exciting frequencies. They used the finite element method to model the wall and compared the results obtained with those of the experiments, which showed that walls with varying height through the length of it have resonance frequencies that appear in the length of the wall. They finally concluded that it is better to analyze the soil-wall system in the 3D domain while calculating the fundamental frequency.

Bathurst and Hatami [9], Hatami and Bathurst [10], EL-Emam and Bathurst [11], Zarnani et al. [12], Ehrilch and Mirmoradi [13], Wang et al. [14], Balakrishnan and Viswanadham [15] and Yazdani et al. [16] used numerical modeling and experimental testing of a geosynthetic reinforced

[DOR: 20.1001.1.22286837.1398.13.5.1.0]

soil retaining wall to analyze the effect of parameters such as wall height, soil backfill width, reinforcement stiffness and length, internal friction angle of the backfill, and toe abutment condition on the seismic behavior of the wall. The results showed that the fundamental frequency of a reinforced soil wall with wide backfill can be calculated with acceptable accuracy using the analytical expressions based on wall height and the domain shear wave velocity. They also showed that the effect of reinforcement stiffness and length and toe abutment condition on the fundamental frequency of the wall is negligible. Bathurst and Hatami [9] and Hatami and Bathurst [10] studied input ground motion, especially the effect of the uniform vertical ground motion and rocking ground motion, on the dynamic behavior of a geosynthetic reinforced soil retaining wall.

Ghanbari et al. [17] proposed an analytical expression for calculating the fundamental frequency of a retaining wall by modeling the wall as a beam and modeling the soil as a set of parallel springs and by invoking the approximate Rayleigh method. Abbasi et al. [18] used the Rayleigh method, modeled the reinforcements as tensional springs to study the effect of the reinforcements on the fundamental frequency of the reinforced soil wall and proposed an analytical expression to calculate its fundamental frequency.

Ramezani et al. [19] investigated the effect of the foundation on the natural frequency of rigid and flexible modes of GRS-FHR walls by using the Rayleigh-Ritz method. In their study, the effect of rocking and translational vibration on the fundamental frequency of the GRS-FHR wall was considered. In their study, because of the 2D analysis, in-depth transverse modes were neglected and the different behaviors of the soil

[DOR: 20.1001.1.22286837.1398.13.5.1.0]

under tension and compression were ignored.

Numerous investigations have also been conducted to study the dynamic and static behavior of the reinforced soil-wall and Masonry and RC wall systems, including: Li and Aguilar [20], Gazetas et al. [21], Tang and Yeh [22], Mojallal et al. [23], Chen et al. [24], Helwaniy et al. [25], Shekarian et al. [26], Ahmadabadi and Ghanbari [27], Ma, Wang et al. [28] and Lin, Liu et al. [29]

Assumptions and Theory

Regarding the proposed method, the following assumptions are considered:

1. The retaining wall is assumed to be clamped-free, flexible and with a constant cross-section area.
2. The backfill is granular, dry, massless and with a constant Young's modulus throughout the entire layer length. Most researchers assume the backfill to be massless to simplify the problem.
3. The backfill is modeled by using a set of axial springs in the back of the wall with constant stiffness.
4. The reinforcements are modeled by using a set of linear continuous axial springs (Figure 2).
5. The plate vibration theory is adopted to analyze the 3D behavior of the retaining wall. Generally, the backfill and the reinforcements are assumed to be linear; all the results obtained in this paper are based on this assumption.
6. The Rayleigh method is used to calculate the fundamental frequency of the retaining wall.

The equation of motion of a rectangular plate is as follows (Rao [30])

[DOR: 20.1001.1.22286837.1398.13.5.1.0]

$$D\left(\frac{\partial^4 w}{\partial x^4}+\frac{\partial^4 w}{\partial y^4}+2\frac{\partial^4 w}{\partial x^2 \partial y^2}\right)+\rho h\frac{\partial^2 w}{\partial t^2}=0 \quad (1)$$

The variational method can be adopted to directly solve equation (1), but it is complicated and time consuming. Meanwhile, the above equation can be solved using the approximate methods to obtain the fundamental frequency, considering the boundary conditions

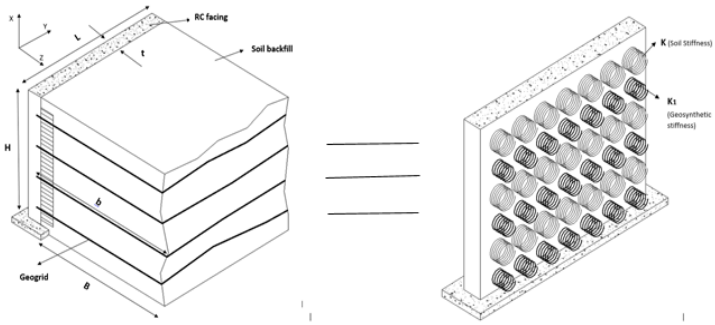

Figure 2. Modeling the interaction between the wall and soil-reinforcements using springs

Some of the approximate methods applicable in this case are the Rayleigh method, Rayleigh-Ritz method, assumed mode method and Galerkin method. Rayleigh [31] showed that based on the energy conservation theory, the obtained fundamental frequency of a mechanical system is either equal to or greater than the real fundamental frequency of the system when using the corresponding shape function. In this method, the fundamental frequency can be obtained by equating the maximum strain and kinetic energy with the continuous system assumptions. The obtained expression is considered as a Rayleigh quotient for continuous systems. Note that in the Rayleigh method, choosing a suitable shape function by considering the interaction between the wall and the backfill is

[DOR: 20.1001.1.22286837.1398.13.5.1.0]

one of the main steps in obtaining the fundamental frequency. Thus, the more the shape function behaves similar to a real wall-soil system, the closer the obtained frequency is to the real fundamental frequency of the system

Proposed Method

In this section, the following equation is used to calculate the maximum kinetic and strain energy by invoking the plate vibration theory. The density of the strain energy, π_0, is as follows (Rao [30])

$$\pi_0=\frac{1}{2}(\sigma_{xx}\varepsilon_{xx}+\sigma_{yy}\varepsilon_{yy}+\sigma_{xy}\varepsilon_{xy}) \tag{2}$$

where σ and ε are stress and strain in the plate, respectively. The strain components are also expressed as a function of transverse displacement parameter $w(x,y)$. Next, by using the stress-strain relation, the stress relation is obtained as a function of $w(x,y)$. Finally, by substituting the recently obtained expressions into equation (2) and integrating over the total volume of the plate, the expression of maximum strain energy of the plate is calculated as

$$U_{\max}=\frac{1}{2}D\int_0^H\int_0^L\{\left(\frac{\partial^2}{\partial x^2}w(x,y)\right)^2+\left(\frac{\partial^2}{\partial y^2}w(x,y)\right)^2+ 2\nu\left(\frac{\partial^2}{\partial x^2}w(x,y)\right)\frac{\partial^2}{\partial y^2}w(x,y)+2(1-\nu)\left(\frac{\partial^2}{\partial y\partial x}w(x,y)\right)^2\}\mathrm{d}x\mathrm{d}y \tag{3}$$

and the maximum kinetic energy can be written as

$$T_{\max}=\frac{1}{2}\frac{\rho t\omega^2}{g}\int_0^b\int_0^a\left(w(x,y)\right)^2\mathrm{d}x\mathrm{d}y \tag{4}$$

where ρ,t,g and ω are plate density, plate thickness, gravitational acceleration and the circular frequency, respectively. The plate stiffness, which is represented by D, can be obtained as

[DOR: 20.1001.1.22286837.1398.13.5.1.0]

$$D=\frac{Et^3}{12(1-\nu^2)} \tag{5}$$

where ν is Poisson's ratio and E is Young's modulus of the plate material.

The shape function $w(x,y)$, which is the product of two perpendicular beams' shape functions, considering the boundary condition of the plate, is obtained as follows (Equation (6)) (Warburton [32])

$$w(x,y)=\theta(x)\theta(y) \tag{6}$$

where $\theta(x)$ and $\theta(y)$ are the corresponding shape functions in the x and y directions, respectively. To model the behavior of the plate, considering the boundary condition, one beam has to be clamped-free and the other has to be free-free because the plate is assumed to be a cantilever. The clamped-free beam shape function is as follows (Warburton [32])

$$\theta(x)=\left(\cos\left(\frac{\gamma x}{H}\right)-\cosh\left(\frac{\gamma x}{H}\right)-k\left(\sin\left(\frac{\gamma x}{H}\right)-\sinh\left(\frac{\gamma x}{H}\right)\right)\right) \tag{7}$$

where

$$k=\frac{\sin\gamma-\sinh\gamma}{\cos\gamma-\cosh\gamma} \tag{8}$$

and

$$\cos\gamma\cosh\gamma=-1 \tag{9}$$

For the free-free beam, the following relation is used

$$\theta(y)=1 \quad for\ m=0 \tag{10}$$

$$\theta(y)=1-\frac{2y}{L} \quad for\ m=1 \tag{11}$$

$$\theta(y)=\cos\gamma'\left(\frac{y}{L}-\frac{1}{2}\right)+k'\cosh\gamma'\left(\frac{y}{L}-\frac{1}{2}\right) \quad \text{for m=2,4,6,.....} \tag{12}$$

Where

$$k'=-\frac{\sin\left(\frac{1}{2}\gamma'\right)}{\sinh\left(\frac{1}{2}\gamma'\right)} \tag{13}$$

and

$$\tan\left(\frac{1}{2}\gamma'\right)+\tanh\left(\frac{1}{2}\gamma'\right)=0 \tag{14}$$

and also

[DOR: 20.1001.1.22286837.1398.13.5.1.0]

$$\theta(y)=\sin\gamma''(\frac{y}{L}-\frac{1}{2})+k''\sinh\gamma''(\frac{y}{L}-\frac{1}{2}) \quad \text{for m=3,5,7,.....} \tag{15}$$

in which

$$k''=\frac{\sin\frac{1}{2}\gamma''}{\sinh\frac{1}{2}\gamma''} \tag{16}$$

γ' is calculated as follows

$$\tan(\frac{1}{2}\gamma'') - \tanh(\frac{1}{2}\gamma'') = 0 \tag{17}$$

m is the number of nodal lines in the vibrating plate, which shows the nodes' positions in the plate of vibration (Warburton [32]).

Now, by dividing the maximum strain energy by the maximum kinetic energy of the system and using the Rayleigh quotient, ω^2 is obtained as

$$U_{\max}=T_{\max}\rightarrow\omega^2=minR(Y(x))=\frac{U_{\max}}{T_{\max}} \tag{18}$$

Where $R(y(x))$, i.e., the Rayleigh quotient, is

$$\omega^2=\frac{U_{\max}+\frac{1}{2}k_1\int_0^L\int_0^H\left(w(x,y)\right)^2 dxdy+\frac{1}{2}\sum_1^i k_2\int_0^L w(x,y)^2 dy}{T_{\max}} \tag{19}$$

The second and third terms in the numerator of equation (19) are the translational springs' energy. They are used to calculate the soil and reinforcement energy, respectively. In the above expressions, k_1 is the soil stiffness per unit area of the plate, which can be calculated using the subgrade modulus. Table 1 shows the expressions for calculating the subgrade reaction coefficient carried out by different researchers thus far. In this article, Vlassov and Leontiev`s [33] relation is used.

Table 1. Different correlations for subgrade reaction modulus proposed by previous researchers

[DOR: 20.1001.1.22286837.1398.13.5.1.0]

Formula	Researcher	
$k_1=\frac{\pi E_S}{2b(1-\nu_S^2)\log(L/B)}$	Galin [34]	E_S=Soil Modules of Elasticity ν_S=Soil Possion Ratio B=Thickness of Layer L=Beam Length b=Beam width
$k_1=\frac{0.65E_S}{b(1-\nu_S)}[\frac{E_S b^4}{E_b I}]\frac{1}{12}$	Vesic and Johnson [35]	E_S=Soil Modules of Elasticity b=Beam width E_b=Beam Modules of Elasticity ν_S=Soil Possion Ratio I=Moment of Inertia
$k_1=\frac{E_S}{B(1+\nu_S)(1-2\nu_S)}$	Vlassov and Leontiev [33]	B=Thikness of Layer ν_S=Soil Possion Ratio E_S=Soil Modules of Elasticity
$k_1=\frac{0.65E_S}{b(1-\nu_S^2)}$	Barden [36]	E_S=Soil Modules of Elasticity ν_S=Soil Possion Ratio b=Beam width
$k_1=\frac{4Es(1-\nu s)}{B(1+\nu_s)(1-2\nu_s}$	Scott [4]	E_S=Soil Modules of Elasticity B=Thikness of Layer ν_S=Soil Possion Ratio
$k_1=1.2E_S$	Makris and Gazetas [37]	E_S=Soil Modules of Elasticity
$k_1=\frac{C_2G}{B}$	Richard *et al.[38]*	B=Thikness of Layer G=Shear modulus C2 = Lumps all The Geometric Variables

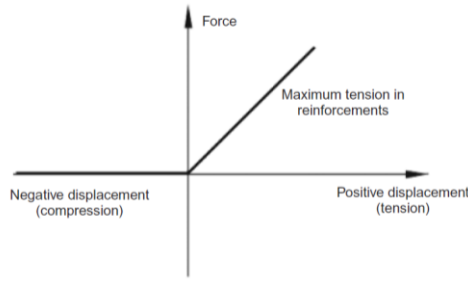

Figure 3. Force-displacement diagram for reinforcement in analytical solution

[DOR: 20.1001.1.22286837.1398.13.5.1.0]

The term k_2 in equation (19) is the stiffness of the reinforcement, which can be calculated using equation (20), considering that it reacts only under tension.

$$k_2=\frac{E_G a}{b} \tag{20}$$

where E_G the is reinforcement elastic modulus, a is the reinforcement cross section area and b is the reinforcement length. Equation (20) has no limitation on the reinforcements' position pattern, which means that they can be attached to the wall with any desirable pattern. The most challenging part of the reinforced walls analytical modeling is that the reinforcements have to be modeled such that they can react only under tension with no reaction under compression. Figure 3 shows the force versus reinforcement displacement diagram.

First, it must be determined in each half cycle of each the three first modes what percentage of each reinforcement's length is under tension and what percentage is under compression. Thus, the reinforcements presented in the analytical model shown in Figure 2 can be modeled such that they only react under tension.

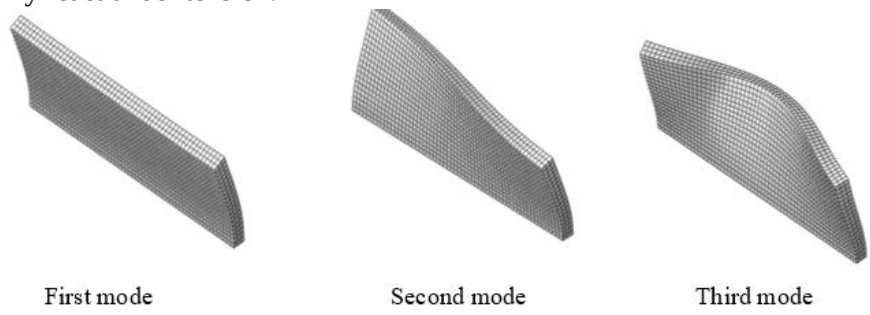

Figure 4. The first three modes of vibration of the retaining walls

As shown in Figure 4, in the first mode, the wall's reinforcements are completely either under tension or under compression, i.e., one hundred

[DOR: 20.1001.1.22286837.1398.13.5.1.0]

percent. Thus, in this case, all the reinforcements are under tension in the first half cycle and under compression in the second half cycle. Thus, their effect is considered only in the first half cycle, where the reinforcements are all under tension. To obtain the total period of the geosynthetic reinforced soil walls, with reinforcements acting only under tension, equation (21) is used.

$$T=\frac{T_1}{2}+\frac{T_2}{2} \tag{21}$$

T_1 and T_2 are the vibration period of the wall with and without the reinforcement's effect, respectively, and T is the total amount of the geosynthetic reinforced soil wall's vibration period, with reinforcements acting only under tension. The circular natural frequency of the wall can be obtained using equation (21) as follows

$$\omega=\frac{2\omega_1\omega_2}{\omega_1+\omega_2} \tag{22}$$

Now, equation (22) can be written for a free natural frequency as equation (23), in which f_t and f_c are the wall's free vibration natural frequency with and without the reinforcements, respectively. f^* is the natural frequency of the wall with tensional reinforcements (Chati et al. [39]).

$$f^*=\frac{2(f_t.f_c)}{f_t+f_c} \tag{23}$$

Thus, for the first mode, f_c, f_t and consequently f^* are obtained by substituting a suitable shape function into equations (3)-(4) and finally by substituting the results into equation (19). Note that when calculating f_t, the effect of the reinforcements is considered, while when calculating f_c, the third term in the numerator of equation (19), which depicts the effect of the reinforcements, is neglected. All the calculations performed in this

[DOR: 20.1001.1.22286837.1398.13.5.1.0]

paper are based on a certain pattern for the reinforcement's position: four reinforcements attached at four different heights, which are $\frac{1}{4},\frac{2}{4},\frac{3}{4}$ and $\frac{4}{4}$ of the wall's height.

$$f_t=\sqrt{\frac{g}{H^4 t\rho}\left(0.025k_1 H^4+0.16k_2 H^3+0.3D\right)} \quad (24)$$

$$f_c=\sqrt{\frac{g}{H^4 t\rho}\left(0.025k_1 H^4+0.3D\right)} \quad (25)$$

where H,t,ρ and g are the height of the wall, wall thickness, wall density and the gravitational acceleration, respectively. The same procedure is considered for the second mode, in which the second mode appears in the length of the wall. Actually, this mode is the one that cannot be studied using 2D modeling. As Figure 4 shows, in each half cycle, a certain part of each reinforcement is under tension. As mentioned earlier, the shape function used in equations (3) and (4) is the product of two perpendicular beams' shape functions. Thus, the free-free beam shape function, which was used in the y direction, can be utilized here again to determine the percentage of each reinforcement's length, which are under tension in each half cycle (Figure 5).

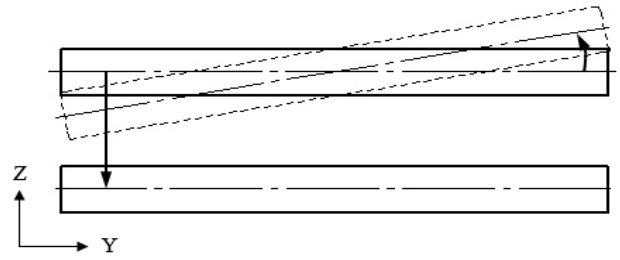

Figure 5. Free-free beam mode shape used in the second mode of the wall's vibration

As shown in Figure 5, during the first half cycle, half of each reinforcement`s length is under tension, while during the second half cycle, the other half of each reinforcement`s length is under tension; thus, in each

[DOR: 20.1001.1.22286837.1398.13.5.1.0]

half cycle, only half of each reinforcement acts. Now f_c and f_t can be calculated using the following equations, considering the tensional share of each reinforcement.

$$f_t = \sqrt{\frac{g}{H^4 L^2 t\rho}\left(0.025 k_1 L^2 H^4 + 0.08 k_2 L^2 H^3 - 2.8 Dv H^2 + 2.8 DH^2 + 0.31 DL^2\right)} \quad (26)$$

$$f_c = \sqrt{\frac{g}{H^4 L^2 t\rho}\left(0.025 k_1 L^2 H^4 + 0.08 k_2 L^2 H^3 - 2.8 Dv H^2 + 2.8 DH^2 + 0.31 DL^2\right)} \quad (27)$$

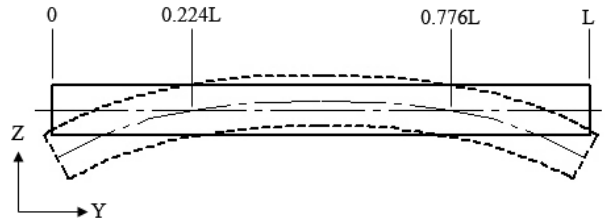

Figure 6. Free-free beam mode shape used in the third mode of the wall's vibration

As Figure 6 shows, which is for the third mode, during the first half cycle, a certain share of the reinforcement is under tension, while during the other half cycle, the remaining share is under tension. As shown in Figure 6, during one half cycle, an approximate share of the wall's length (y-axis), i.e., from $0.224l$ to $0.776l$, is under tension, while during the other half cycle, the remaining shares, i.e., from 0 to $0.224l$ and from $0.776l$ to l, together are under tension.

f_c and f_t are now obtained as follows, considering the assumptions considered for the third mode.

$$f_t = \sqrt{\frac{g}{H^4 L^4 t\rho}\left(\begin{matrix}0.025 k_1 H^4 L^4 + 0.048 k_2 L^4 H^3 - 4.7 Dv H^2 L^2 + \\ 12.68 DH^4 + 9.24 DH^2 L^2 + 2.4 DL^4\end{matrix}\right)} \quad (28)$$

$$f_c = \sqrt{\frac{g}{H^4 L^4 t\rho}\left(\begin{matrix}0.025 k_1 H^4 L^4 + 0.067 k_2 L^4 H^3 - 4.74 Dv H^2 L^2 + \\ 12.68 DL^4 + 9.24 DH^2 L^2 + 2.4 DL^4\end{matrix}\right)} \quad (29)$$

where f_t is the natural frequency of the wall when the middle share of

[DOR: 20.1001.1.22286837.1398.13.5.1.0]

the wall is under tension (i.e., $_{0.2241–0.7761}$) and f_c is the natural frequency of the wall while the remaining part of the wall is under tension.

Finally, by substituting the obtained f_c and f_t for each of the three modes in equation (23), the natural frequency of the geosynthetic reinforced soil wall, with reinforcements acting only under tension, is obtained.

Comparison of analytical solution with that of other researchers and finite element method

In this section, the results achieved by the proposed method are compared with the ones obtained by other researchers and the finite element method.

First, the effect of the reinforced soil wall's height on the frequency is illustrated in Figure 7, As shown, as the reinforced soil wall's height increases, the fundamental frequency of the system decreases due to the wall's softening. The material properties used in this section are presented in Table 2.

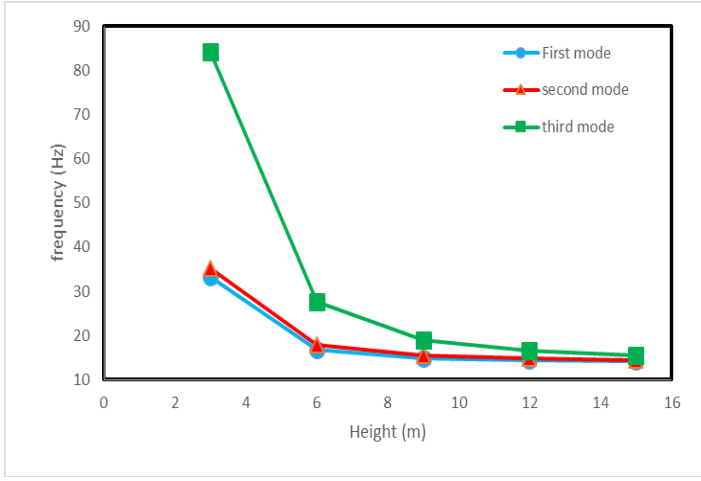

Figure 7. Variation of effective natural frequency versus the height of

[DOR: 20.1001.1.22286837.1398.13.5.1.0]

the GRS-FHR wall

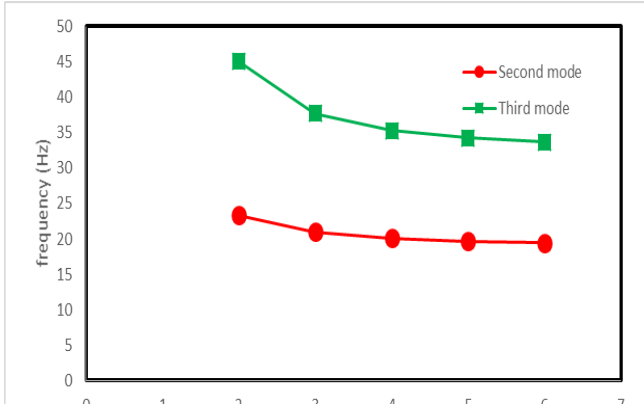

Figure 8. Variation of effective natural frequency versus length to height ratio of the wall

Table 2. Material properties used in this section

Soil		Geosynthetic		Wall	
B	5 (m)	b	5 (m)	H	**5 (m)**
E_s	30 (MPa)	E_r	3000 (MPa)	E_c	**23500 (MPa)**
ν_s	0.2	ν_r	0.2	ν_c	**0.2**
		a	0.01 (m^2)	L	**20 (m)**

Figure 8 shows the effect of length to height ratio variation on the fundamental frequency of the wall in the second and third mode. As can be understood from the expressions presented so far, in contrast to the second and the third mode, the length of the wall does not affect the fundamental frequency of the wall in the first mode. As the length to height ratio of the wall increases, the fundamental frequency of the wall decreases, indicating that the stiffness decreases when the length to height ratio increases

In the following, the effect of parameters, such as the thickness to height ratio and reinforcement to soil stiffness ratio variation, on the fundamental frequency of the wall will be studied in the first three modes.

[DOR: 20.1001.1.22286837.1398.13.5.1.0]

As shown in Table 3, when the thickness to height ratio increases or, namely, when the wall becomes stiffer, the effect of the reinforcement to soil stiffness ratio on the wall's fundamental frequency decreases. Actually, the stiffer the wall's face becomes, the less the reinforcements affect the wall's fundamental frequency and vice-versa. The results presented in Table 3 are for a wall 6 meters high and 12 meters long

Table 3. Effect of thickness to height ratio and reinforcement to soil stiffness ratio variation on the effective fundamental frequency of the wall in the first three modes

Mode Number	**1**			**2**			**3**		
K_2/k_1 **t/H**	0.1	0.5	1	0.1	0.5	1	0.1	0.5	1
0.02	13.53	14.57	15.52	14.8	15.97	17.32	15	16.2	17.6
0.05	13.9	14.93	15.88	15.75	16.8	18.13	17.1	18.2	19.42
0.08	15.07	16.05	16.9	18.52	19.46	20.58	22.1	23	24
0.11	17.29	18.18	19.1	23.33	24.1	25	29.5	30.2	31
0.14	20.56	21.34	22.2	29.85	30.45	31.2	38.8	39.37	40
0.17	24.76	25.43	26.2	37.73	38.2	38.8	49.8	50.2	50.7
0.2	29.7	30.3	30.95	46.71	47.1	47.57	62.1	62.44	62.87

This section aims to study the effect of utilizing the reinforcements and the effect of different behaviors of reinforcements under tension and compression on the fundamental frequency of the retaining wall.

The fundamental frequencies presented in Table 4 can be categorized in the following three groups: 1. No reinforcement utilized; 2. Reinforcements utilized, considering the effective behavior (no compression); 3. Reinforcement utilized, reacting both under tension and compression.

[DOR: 20.1001.1.22286837.1398.13.5.1.0]

The results presented in Table 4 are obtained using the material introduced in Table 2 for a wall 30 meters long, 9 meters high and 0.5 meter thick. As Table 4 depicts, reinforcements reacting only under tension can affect the fundamental frequency and change it by approximately 10 to 15 percent in comparison with the reinforcements that react both under tension and compression.

Table 4. Fundamental frequency of the wall based on three different cases for the reinforcements

	First mode (Hz)		
E_g (Reinforcement elastic modulus) (MPa)	No reinforcement	Effective reinforcement	Full behavior reinforcement
1000	13.55	14.04	14.57
2000	13.55	14.47	15.53
3000	13.55	14.85	16.43
4000	13.55	15.19	17.29
	Second mode (Hz)		
1000	13.8	14.3	15
2000	13.8	14.8	15.9
3000	13.8	15.27	16.86
4000	13.8	15.7	17.72
	Third mode (Hz)		
1000	14.8	15.3	15.79
2000	14.8	15.7	16.7
3000	14.8	16.3	17.6
4000	14.8	16.7	18.43

Next, the results obtained using the proposed method will be compared with the results of the finite element method. The finite element software Abaqus was used to model the reinforced soil wall. A C3D8R element (a 3D-8 node linear brick reduced integration) was used for modeling the wall, while a S4R (a 4 node doubly curved thin or thick shell, reduced integration) was utilized to model the reinforcements.

Note that the material used in the shell was active only under tension. For the tangential behavior of the soil interaction, the penalty formulation had a friction coefficient of 0.32; for normal behavior, hard contact was

[DOR: 20.1001.1.22286837.1398.13.5.1.0]

used for pressure-overclosure. To consider the interaction between soil, reinforcement and the wall, the shell element was embedded in the soil and was attached to the wall using the tie constraint (shell to surface).

As shown in Figure 9, the effect of the soil stiffness (k_1) to wall rigidity (D) ratio variation, which is called the stiffness ratio, on the wall's fundamental frequency is investigated

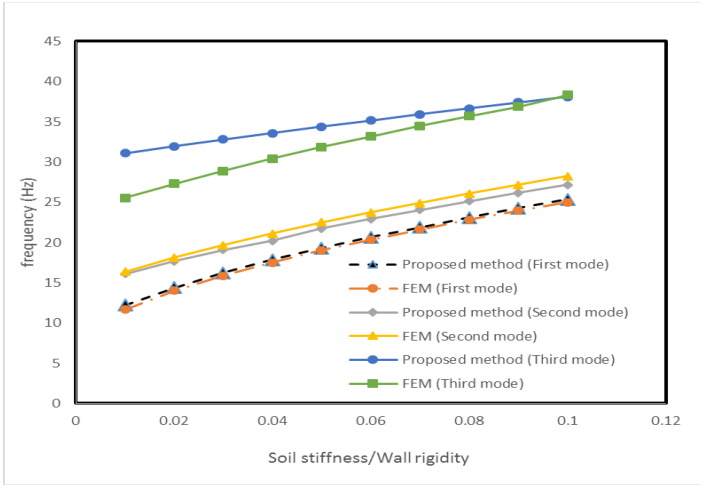

Figure 9. Variation of effective fundamental frequency of the wall against stiffness ratio

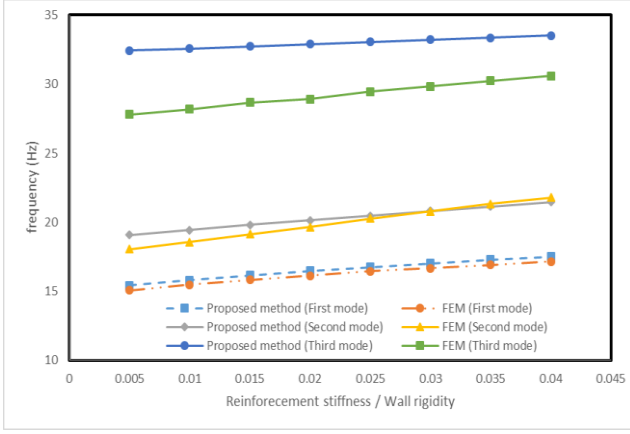

Figure 10. Three first modes of the effective fundamental frequencies

[DOR: 20.1001.1.22286837.1398.13.5.1.0]

variation of the wall versus

Figure 10 shows the effect of the reinforcement stiffness (k_2) to wall rigidity (D) ratio variation on the wall's three first mode frequencies.

Finally, variation of the first three modes' effective fundamental frequency against the reinforcement stiffness (k_2) to soil stiffness (k_1) ratio is shown in Figure 11. Increasing the reinforcement to soil stiffness ratio causes the fundamental frequency to increase. In Figures 9, 10 and 11, the height, length and width of the backfill are assumed to be 12, 6 and 5 meters, respectively.

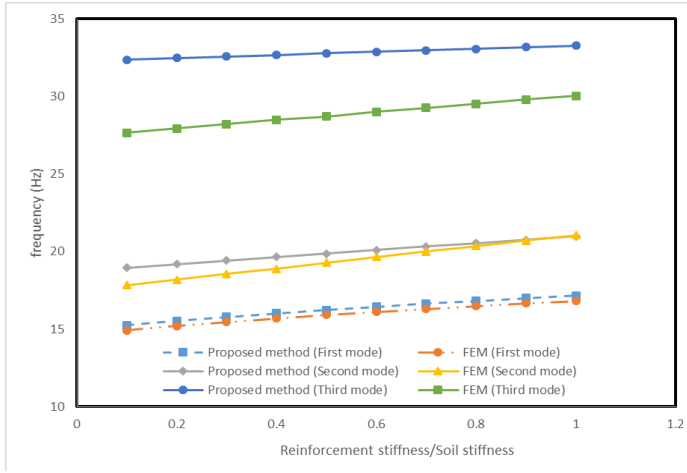

Figure 11. Variation of effective fundamental frequency of the wall against reinforcement stiffness to soil stiffness ratio

As Figure 11 demonstrates, the results of the proposed method are in good agreement with the results from the finite element method, especially in the first two modes. Increasing the reinforcement to soil stiffness ratio causes the fundamental frequency of the wall to increase.

The proposed method in the first mode is now compared with Abbasi et al. [18] in Table 5. In this section, the parameters are assumed to be as follows

[DOR: 20.1001.1.22286837.1398.13.5.1.0]

$$k_1 = 18e6(^{MN}/_{m}), \quad k_2 = 60e6(^{MN}/_{m}), \quad E_c = 26(Gpa)$$

$$\rho = 2320(^{kg}/_{m^3}), \quad t = 0.075\,H$$

Table 5. Comparison of the first mode frequency obtained by the proposed method and Abbasi et al. [18]

k_1=18e6 MN/m, k_2=60e6 MN/m		
	first mode frequency (Hz)	
length of the wall (m)	Abbasi et al. [18]	proposed method
3	47.4	47.6
5	32.14	33.06
6	28.23	29.28
8	23.2	24.24
10	20.02	20.09

Different behaviour of the soil under tension and compression

In this section, the effect of the different behaviors of the soil under tension and compression on the fundamental frequency of GRS-FHR walls is studied. The equation of Chati et al. [39] is used here again and the vibration's period is divided into two parts. In the first part, a specific portion of the soil is under tension, but not all of it; consequently, in the second part, the remaining portion is under tension. As mentioned before, the interaction between the wall and soil is modeled using springs; thus, in each half cycle, the part of the soil under tension must be specified to neglect that part. Note that the soil's behavior is different from that of the reinforcements, which means that in contrast to the reinforcements, the soil reacts only under compression.

In the first mode, as depicted in Figure 4, in one half cycle, both the backfill and the reinforcements are under tension, while in the other half cycle, all of them are under compression. Thus, in the tensional half cycle,

[DOR: 20.1001.1.22286837.1398.13.5.1.0]

only the effect of the reinforcements is considered in the calculations, while in the compressive half cycle only, the effect of the backfill is considered in the calculations. Finally, the proposed formula for the first mode can be written as follows

$$f_c = \sqrt{\frac{g}{H^4 t\rho}\left(0.025 k_1 H^4 + 0.3D\right)} \quad (30)$$

$$f_t = \sqrt{\frac{g}{H^4 t\rho}\left(0.16 k_2 H^3 + 0.3D\right)} \quad (31)$$

Where in equation (30), which is for the compressive half cycle, the effect of the reinforcements is neglected, and in equation (31), which is for the tensional half cycle, the effect of the backfill is neglected. The fundamental frequency of the reinforced soil retaining wall is obtained using the equation of Chati et al. [39].

The procedure invoked for the first mode can be implemented here again to analyze and distinguish the compressive and tensile behavior of the soil. As shown in Figure 4, in one half cycle of the period, half of the wall's length is under tension and the other half is under compression. Thus, in half of the wall's length, which is under tension, only the reinforcements' effects are considered, while in the other half, which is under compression, only soil reaction is considered

$$f_c = \sqrt{\frac{g}{H^4 L^2 t\rho}\left(\begin{array}{l}0.013 k_1 b^2 a^4 + 0.08 k_2 b^2 a^3 - \\ 2.8 D\nu a^2 + 2.8 D a^2 + 0.31 D b^2\end{array}\right)} \quad (32)$$

$$f_t = \sqrt{\frac{g}{H^4 L^2 t\rho}\left(\begin{array}{l}0.013 k_1 b^2 a^4 + 0.08 k_2 b^2 a^3 \\ -2.8 D\nu a^2 + 2.8 D a^2 + 0.31 D b^2\end{array}\right)} \quad (33)$$

In equations 32 and 33, which are for the second mode, the tensile and compressive behaviors of both the soil and reinforcements are separated. By using the same procedure as for the third mode, equations 34 and 35 can be obtained, which clarify the difference between the compressive and

[DOR: 20.1001.1.22286837.1398.13.5.1.0]

tensile behavior, as in previous modes.

$$f_t=\sqrt{\frac{g}{H^4L^4t\rho}\begin{pmatrix}0.015k_1H^4L^4+0.048k_2L^4H^3-4.74D\nu H^2L^2\\+12.68DH^4+9.24DH^2L^2+2.4DL^4\end{pmatrix}} \quad (34)$$

$$f_c=\sqrt{\frac{g}{H^4L^4t\rho}\begin{pmatrix}0.011k_1H^4L^4+0.07k_2L^4H^3-4.74D\nu H^2L\\2+12.68DH^4+9.24DH^2L^2+2.4DL^4\end{pmatrix}} \quad (35)$$

Table 6 shows the results obtained by the proposed method under two conditions: first, when the compressive behavior is considered for the soil and tensile behavior for the reinforcements; second, when the soil is assumed to act under any condition (i.e., compression or tension) but the reinforcements still only act under tension. The comparison between the results showed that excluding tensile behavior from the soil can reduce the fundamental frequency of the reinforced wall by approximately 20-25 percent. In Table 6, the length and thickness of the wall are 20 and 0.5 meter, respectively, and the elastic modulus of the soil and geosynthetic are 60 and 3000 MPa, respectively.

Table 6. Comparison between tensile-compressive behavior and compressive behavior of the soil

	Considering both tension and compression behavior for soil		
Height (m)	**First mode (Hz)**	**Second mode (Hz)**	**Third mode (Hz)**
3	33.23	34.94	83.8
5	19.5	20.6	35.56
7	17.12	17.78	24
9	16.45	16.87	20.11
	Considering only compression behavior for soil		
Height (m)	**First mode (Hz)**	**Second mode (Hz)**	**Third mode (Hz)**
3	31.38	33.12	83.05
5	15.62	16.62	33.4
7	11.69	12.76	20.5
9	9.98	11.37	15.7

The results obtained using the proposed method are compared with the ones presented by Zarnani et al. [12] to validate them. Zarnani et al. [12] developed a simple numerical FLAC model to simulate the dynamic response of two instrumented, reduced-scale model reinforced soil walls.

[DOR: 20.1001.1.22286837.1398.13.5.1.0]

The models were constructed on a 1-g shaking table, which was implemented by El-Emam and Bathurst (2004; 2005). The models were 1 m high by 1.4 m wide by 2.4 m long and were constructed with a uniform-sized sand backfill. A polymeric geogrid reinforcement material with appropriately scaled stiffness and a structural full-height rigid panel facing were also embedded in the models. El-Emam and Bathurst assumed the shear modules of the soil to be 7 Mpa and reinforcement cross section and elastic modules to be 45000 kPa and 0.002 m^2, respectively. See Zarnani et al. [12] for further details the comparison of the results is presented in Table 7.

Table 7. Comparison of the results from the proposed method and those obtained by Zarnani et al. (2011)

	Proposed method (Hz)	Zarnani et al. [12] (Hz)
Frequency (Hz)	25.1	21

In the following, the results obtained using the proposed method and the results from the full scale experiment performed by Elgamal et al. [8] are compared to verify the proposed method. The experiment performed by Elgamal et al. [8] was for the forced vibration of a non-reinforced retaining wall; thus, the reinforcements are ignored in the proposed method in this section. Elgamal et al. [8] studied the forced vibration of a wall with varying height experimentally to investigate the frequencies of a retaining wall in the 3D domain. Finally, by using finite element modeling, they studied the behavior of a wall with fixed and varying height. The obtained frequencies are presented in Table 7, considering a wall 9 meters high, 0.4 meter thick and 45 meters long. The backfill had a thickness of 36.6 meters, Poisson's ratio of 0.3 and elastic coefficient of 30 MPa. The wall had a Poisson's ratio of 0.15, elastic modulus of 19 GPa and density of 2300 kg/m^3.

[DOR: 20.1001.1.22286837.1398.13.5.1.0]

In the experiments performed by Elgamal et al. [8], for the fixed height case, the results were obtained only for the first two modes, which were excited along the height of the wall. Thus, in Table 7, only the two modes that were mentioned are compared. It shows that the solution obtained using the proposed method in the present paper is in good agreement with the experimental results, consequently confirming the accuracy of the proposed formulation.

Table 8. Comparison of the results of the proposed method with field data obtained by Elgamal et al. (1996)

	First mode frequency (Hz)	Second mode frequency (Hz)
Proposed method	4.3	**14.4**
Elgamal et al. [8]	6	**17.8**

Conclusion Remarks

This paper aimed to obtain an accurate formulation to estimate the first three natural frequencies of flexible geosynthetic-reinforced soil retaining walls with full-height rigid concrete (GRS-FHR) having a fixed cross section based on the theory of plates on an elastic foundation and the energy method in 3D.

Major findings from this study can be summarized as follows:

- In this paper, 3D modeling using the plate element allowed for studying the in-depth transverse modes, which are so important in the dynamic behavior of GRS-FHR walls, while in the 2D analytical modeling performed so far, which used the beam element, this is impossible.
- A new analytical method for 3D vibration of a reinforced retaining wall, considering soil-structure interaction, is proposed.
- In the proposed method, the reinforcements react only under tension. For this purpose, in each of the three modes, the vibration period is

[DOR: 20.1001.1.22286837.1398.13.5.1.0]

divided into two half cycles; in the first half cycle, a specified share of each reinforcement`s length is under tension, while in the second half cycle, the remaining share is under tension. Finally, by using the equations presented in this paper, the effective natural frequency of the system is obtained.

- The results obtained from the proposed method showed that the effect of reinforcements on the fundamental frequency in higher modes decreases. It was also shown that as the wall becomes stiffer, the effect of the reinforcements on the fundamental frequency decreases.
- As demonstrated by the achieved results, considering the real behavior of the reinforcements, which react only under tension, causes the fundamental frequency of the reinforced soil retaining wall to vary from 5 to 10 percent.
- The results showed that considering the difference between the compressive and tensile behavior of soil can cause a near 20-25 percent reduction in the fundamental frequency of the reinforced soil walls.
- The results obtained by the proposed method were in good agreement with the results achieved by the 3D finite element method and field measurements by other researchers, especially in the first two modes.

Conclusion Remarks

This paper aimed to obtain an accurate formulation to estimate the first three natural frequencies of flexible geosynthetic-reinforced soil retaining walls with full-height rigid concrete (GRS-FHR) having a fixed cross section based on the theory of plates on an elastic foundation and the energy method in 3D.

Major findings from this study can be summarized as follows:

- In this paper, 3D modeling using the plate element allowed for

[DOR: 20.1001.1.22286837.1398.13.5.1.0]

studying the in-depth transverse modes, which are so important in the dynamic behavior of GRS-FHR walls, while in the 2D analytical modeling performed so far, which used the beam element, this is impossible.

- A new analytical method for 3D vibration of a reinforced retaining wall, considering soil-structure interaction, is proposed.
- In the proposed method, the reinforcements react only under tension. For this purpose, in each of the three modes, the vibration period is divided into two half cycles; in the first half cycle, a specified share of each reinforcement`s length is under tension, while in the second half cycle, the remaining share is under tension. Finally, by using the equations presented in this paper, the effective natural frequency of the system is obtained.
- The results obtained from the proposed method showed that the effect of reinforcements on the fundamental frequency in higher modes decreases. It was also shown that as the wall becomes stiffer, the effect of the reinforcements on the fundamental frequency decreases.
- As demonstrated by the achieved results, considering the real behavior of the reinforcements, which react only under tension, causes the fundamental frequency of the reinforced soil retaining wall to vary from 5 to 10 percent.
- The results showed that considering the difference between the compressive and tensile behavior of soil can cause a near 20-25 percent reduction in the fundamental frequency of the reinforced soil walls.
- The results obtained by the proposed method were in good agreement with the results achieved by the 3D finite element method and field measurements by other researchers, especially in the first two modes.

[DOR: 20.1001.1.22286837.1398.13.5.1.0]

Basic SI units are given in parentheses.

a	Reinforcement cross section (m^2)
b	Reinforcement length (m)
D	Plate stiffness (Kg.m)
E_g	Reinforcement elastic modulus (MPa)
E, E_c	wall (concrete) Modulus of Elasticity (Pa)
E_s	soil Modulus of Elasticity (Pa)
f_c, f_t	Wall's free vibration natural frequency with and without the reinforcements (Hz)
f^*	Natural frequency of the wall with tensional reinforcements (Hz)
g	Gravitational acceleration (m^2/s)
H	Height of the wall (m)
K_1	Soil stiffness per unit area of the plate (N/m^3)
K_2	axial stiffness of reinforcements (N/m)
L	Length of wall (m)
t	Wall width (m)
U_{max}	Maximum strain energy of the plate (J)
T_{max}	Maximum kinetic energy (J)
T_1, T_2	Vibration period of the wall with and without the reinforcement's effect (Second)
$w(x,y$	Function of transverse displacement of plate (m)
ρ	wall density (kg/m^3)
ρ_s	soil density (kg/m^3)
ν_c	Concrete Poisson's ratio (dimensionless)
ν_G	Geosynthetic Poisson's ratio (dimensionless)
ν_s	soil Poisson's ratio (dimensionless)
ω	natural circular frequency of wall (rad/s)
ε	Strain in plate (dimensionless)
σ	Stress in plate (N/mm^2)
π_0	Density of the strain energy (J)

References

1. Tatsuoka F., Koseki J., Tateyama M., "Performance of reinforced soil structures during the 1995 Hyogo-Ken Nambu earthquake", Special

[DOR: 20.1001.1.22286837.1398.13.5.1.0]

lecture. Proceedings of the International Symposium on Earth Reinforcement (IS Kyushu '96), Balkema, Rotterdam, the Netherlands, No. 2 (1997) 973-1008.

2. Matsuo H., Ohara S., "Lateral earth pressure and stability of quay walls during earthquakes", Proc. of the 2nd World Conf. on Earthquake Engineering, Tokyo-Kyoto, Japan (July 1960).
3. Wood J. H., "Earthquake-induced soil pressures on structures", Ph.D. Dissertation, California Institute of Technology, Pasadena (1973).
4. Scott R. F., "Earthquake-induced earth pressures on retaining walls", Proc. of the5th World Conf. on Earthquake Engineering, Rome, Italy (1973.).
5. Wu G., "Dynamic soil–structure interaction: pile foundations and retaining structures", University of British Columbia, Vancouver (1994.).
6. Yeh C. S., "Dynamic response of retaining walls during earthquake", Proc. International Symposium on Earthquake Structural Engineering, St. Louis, Mo., U.S.A, (1976) 387-92.
7. Jain S. K., Scott R. F., "Seismic analysis of cantilever retaining walls, Transactions of the 10th International Conference on Structural Mechanics in Reactor Technology", Anaheim, USA (1989.) 241-246.
8. Elgamal A., Alampalli S., Laak P., "Forced Vibration of Full-Scale Wall-Backfill System, J. Geotechnical Engeeniring, 122m No. 10, (1996) 849-858.
9. Bathurst R. J., Hatami K., "Seismic response analysis of a geosynthetic reinforced soil retaining wall", J. Geosynthetic International. 5, No. 1-2, (1998) 127-166.
10. Hatami K., Bathurst R. J., "Effect of structural design on fundamental frequency of reinforced soil retaining walls", J. Soil Dynamics and Earthquake Engineering. 19m No. 3 (2000) 137-157.
11. EL-Emam M. M., Bathurst R. J., "Influence of reinforcement

[DOR: 20.1001.1.22286837.1398.13.5.1.0]

parameters on the seismic response of reduced-scale reinforced soil retaining walls", J. Geotextile Geomembrane. 25, No. 1 (2007) 33-49.

12. Zarnani S., El-Emam M. M., Bathurst, R. J., "Comparison of numerical and analytical solutions for reinforced soil wall shaking table test", Geomech. Engineer. No. 3, 291-321.
13. Ehrilch M., Mirmoradi S. H., "Evaluation of the effects of facing stiffness and toe resistance on the behavior of GRS walls", J. Geotextile Geomembrane. 40 (2013) 28-36.
14. Wang L., Chen G., Chen S., "Experimental study on seismic response of geogrid reinforced rigid retaining walls with saturated backfill sand. J. Geotextiles and Geomembranes. 43, No. 1 (2015) 35-45.
15. Balakrishnan S., Viswanadham B. V. S., "Performance evaluation of geogrid reinforced soil walls with marginal backfills through centrifuge model tests", J. Geotextile and Geomembrane. 44m No. 1, (2016) 95-108. 16. Yazdani H., Hatami K., Grady B. P., "Sensor-Enabled Geogrids for Performance Monitoring of Reinforced Soil Structures", ASTM J. Testing and Evaluation. 44, No. 1(2016).
17. Ghanbari A., Hoomaan E., Mojallal M., "An analytycal method for calculating the natural frequency of retaining walls", International Journal of Civil Engineering. No. 1 (2013) 1-9.
18. Abbasi O., Ghanbari A., Hosseini S. A. A., "An analytical method for calculating the natural frequency of reinforced retaining walls with soil structure interaction effect", J. Geosynthetics International. 21, No. 1 (2014) 53-61.
19. Ramezani M. S., "A Ghanbari, and SAA Hosseini", Analytical Method for Calculating Natural Frequencies of Geosynthetic-Reinforced Wall with Full-Height Concrete Facing" Geosynthetics International (2016) 1-13.
20. Liu H., Wang X., Song E., "Long-term behavior of GRS retaining walls with marginal backfill soils", J. Geotextiles and Geomembranes, 27m

[DOR: 20.1001.1.22286837.1398.13.5.1.0]

No. 4 (2009) 295-307.

21. Gazetas G., Psarropoulos P. N., Anastasopoulos I., Gerolymos N., "Seismic behavior of flexible retaining systems subjected to short-duration moderately strong excitation", J. Soil Dynamics and Earthquake Engineering. 24, No 7 (2004) 537-550.
22. Tang Yu, Chau-Shioung Yeh., "A Note on the Seismic Response of Rigid Cantilever Retaining Walls", Nuclear Engineering and Design 241, No. 3 (2011) 693-99.
23. Mojallal M., Ghanbari A., "Prediction of seismic displacements in gravity retaining walls based on limit analysis approach", J. Structural Engineering and Mechanics. 42, No. 2. (2012).

DOI 10.12989/sem.2012.42.2.247

24. Chen J. F., Tolooiyan A., Xue J. F., Shi Z. M., "Performance of a geogrid reinforced soil wall on PVD drained multilayer soft soils", J. Geotextiles and Geomembranes. *44, No. 3* (2016) 219-229.
25. Helwany S. M. B., Reardon G., Wu J. T. H., "Effects of backfill on the performance of GRS retaining walls", J. Geotextiles and Geomembranes, 17, No. 1 (1999) 1-16.
26. Shekarian S., Ghanbari A., Farhadi A., "New seismic parameters in the analysis of retaining walls with reinforced backfill", J. Geotextile and Geomembrane. 26, No. 4 (2008) 350-356.
27. Ahmadabadi M., Ghanbari A., "New procedure for active earth pressure calculation in retaining walls with reinforced cohesive-frictional backfill", J. Geotextiles and Geomembranes, 27, No.6 (2009) 456-463.
28. Ma S. j., et al., "Pseudo-dynamic active earth pressure behind retaining wall for cohesive soil backfill", Journal of Central South University 19 (2012) 3298-3304.
29. Lin Y.-l., et al., "Dynamic response law about gravity retaining wall to seismic characteristics and earth fill properties", Journal of Central South University **19** (2012) 657-663.

30. Rao S. S., "Vibration of Continuous Systems", John Wiley & Sons, New Jersey, NJ, USA (2007).
31. Rayleigh J. W. S., Lindsay R. B., "Theory of Sound, (vol. 1,2nd Edition)", Macmillan and Co., London, England (1894).
32. Warburton G. B., "The vibration of rectangular plates", Proc. of the Institute of Mechanical Engineering (June 1954).
33. Vlassov V. Z., Leontiev N. N., "Beams, plates and shells on an elastic foundation", Moscow, USSR: Fizmatgiz, (1960) (in Russian).
34. Galin L. A., "On the Winkler-Zimmermann hypothesis for beams", J. Prikl. Mat. Mekh. 7, No. 4 (1943) 293-300 (in Russian)
35. Vesic A. B., Johnson W. H., "Model studies of beams resting on a silt subgrade, Proceeding of ASCE. J. Soil Mechanic and Foundation, 89 (1963) 1-31.
36. Barden L., "The Winkler model and its application to soil", J. Structure Engineering, 41(1963) 279-280.
37. Makris N., Gazetas G., "Dynamic Pile-Soil-Pile Interaction, Part 11: Lateral and seismic response", Earthquake Engineering and Structural Dynamics; 21 (1992) 145-62. DOI 10.1002/eqe.4290200203
38. Richards Jr, R., Huang C., Fishman K. L., "Seismic earth pressure on retaining structures", J. Geotechnical and Geoenvironmental Engineering, 125, No. 9 (1999) 771-778.
39. Chati M., Rand R., Mukherjee S., "Modal analysis of a cracked beam", Journal of Sound and Vibration, 207, No. 2 (1997) 249-27

[DOR: 20.1001.1.22286837.1398.13.5.1.0]